# Crystal Structure of the Pyocyanin Biosynthetic Protein PhzS[†,‡]

Bryan T. Greenhagen,[§] Katherine Shi,[§] Howard Robinson,[#] Swarna Gamage,[⊥] Asim K. Bera,[§] Jane E. Ladner,*[,§,||] and James F. Parsons*[,§]

*Center for Advanced Research in Biotechnology, University of Maryland Biotechnology Institute, National Institute of Standards and Technology, 9600 Gudelsky Drive Rockville, Maryland 20850, Auckland Cancer Society Research Centre, School of Medicine, Faculty of Medical and Health Sciences, University Of Auckland, Auckland, New Zealand, and Biology Department, Brookhaven National Laboratory, Upton, New York 11973-5000*

*Received December 19, 2007; Revised Manuscript Received March 17, 2008*

ABSTRACT: The human pathogen *Pseudomonas aeruginosa* produces pyocyanin, a blue-pigmented phenazine derivative, which is known to play a role in virulence. Pyocyanin is produced from chorismic acid via the phenazine pathway, nine proteins encoded by a gene cluster. Phenazine-1-carboxylic acid, the initial phenazine formed, is converted to pyocyanin in two steps that are catalyzed by the enzymes PhzM and PhzS. PhzM is an adenosylmethionine dependent methyltransferase, and PhzS is a flavin dependent hydroxylase. It has been shown that PhzM is only active in the physical presence of PhzS, suggesting that a protein−protein interaction is involved in pyocyanin formation. Such a complex would prevent the release of 5-methyl-phenazine-1-carboxylate, the putative intermediate, and an apparently unstable compound. Here, we describe the three-dimensional structure of PhzS, solved by single anomalous dispersion, at a resolution of 2.4 Å. The structure reveals that PhzS is a member of the family of aromatic hydroxylases characterized by *p*-hydroxybenzoate hydroxylase. The flavin cofactor of PhzS is in the solvent exposed out orientation typically seen in unliganded aromatic hydroxylases. The PhzS flavin, however, appears to be held in a strained conformation by a combination of stacking interactions and hydrogen bonds. The structure suggests that access to the active site is gained via a tunnel on the opposite side of the protein from where the flavin is exposed. The C-terminal 23 residues are disordered as no electron density is present for these atoms. The probable location of the C-terminus, near the substrate access tunnel, suggests that it may be involved in substrate binding as has been shown for another structural homologue, RebC. This region also may be an element of a PhzM−PhzS interface. Aromatic hydroxylases have been shown to catalyze electrophilic substitution reactions on activated substrates. The putative PhzS substrate, however, is electron deficient and unlikely to act as a nucleophile, suggesting that PhzS may use a different mechanism than its structural relatives.

Pyocyanin is a phenazine pigment produced by *Pseudomonas aeruginosa.* As early as 1860, it was appreciated that a blue pigment could be extracted from certain bacterial cultures, and prior to 1900, it was known that old cultures of *Pseudomonas* contained substances highly toxic to other bacteria (*1*). Phenazines are now known to be a diverse class of secondary metabolites produced by *Pseudomonas*, *Streptomyces*, and other bacterial species. They range from simple tricyclic structures such as pyocyanin to elaborate molecules such as the esmeraldines (*2, 3*). Many phenazines have been shown to impact important biological processes, and some have antimicrobial properties that producing strains use to their competitive advantage (*4*).

Pyocyanin imparts the characteristic blue or blue-green color to *P. aeruginosa* cultures and to fluids such as lung sputum from cystic fibrosis patients. A number of recent studies have shown that pyocyanin produced by *P. aeruginosa* plays a significant role in virulence (*5*−*9*). In order to evaluate whether inhibition of pyocyanin biosynthesis could be a clinically feasible option in combating *P. aeruginosa*, a serious nosocomial pathogen, we have undertaken a structural and mechanistic analysis of the proteins involved in phenazine biosynthesis (*10*−*13*).

Phenazines are synthesized from chorismic acid in *P. aeruginosa* by the products of the *phzABCDEFG* operon

[†] This work was supported by NIH Grant AI067530 (to J.F.P.). Some data for this study were measured at beamline X29 of the National Synchrotron Light Source. Financial support comes principally from the Offices of Biological and Environmental Research and of Basic Energy Sciences of the U.S. Department of Energy, and from the National Center for Research Resources of the National Institutes of Health.

[‡] Coordinates for PhzS have been deposited in the RCSB Protein Data Bank as entry 2RGJ.

* To whom correspondence should be addressed. Center for Advanced Research in Biotechnology, 9600 Gudelsky Drive, Rockville, Maryland 20850. (J.F.P.) Phone: 240-314-6158. Fax: 240-314-6255. E-mail: parsonsj@umbi.umd.edu. (J.E.L.) E-mail: jane.ladner@nist.gov.

[§] Center for Advanced Research in Biotechnology.

[||] National Institute of Standards and Technology.

[⊥] University of Auckland.

[#] Brookhaven National Laboratory.

[1] Abbreviations: PCA, phenazine-1-carboxylate; 5-methyl-PCA, 5-methylphenazine-1-carboxylate; PHBH, *para*-hydroxybenzoate hydroxylase; 3HBH, 3-hydroxybenzoate hydroxylase; DTT, dithiothreitol; FAD, flavin adenine dinucleotide; SeMet, selenomethionine; SAM, *S*-adenosylmethionine; SAD, single anomalous dispersion; TFA, trifluoroacetic acid.

10.1021/bi702480t CCC: $40.75 
Published on Web 04/17/2008

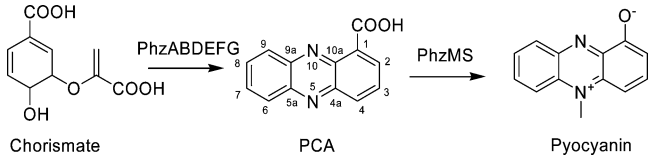


FIGURE 1: Biosynthetic pathway leading to pyocyanin in *P. aeruginosa*.

(Figure 1). The initial aromatic product, phenazine-1-carboxylate (PCA[1]), is converted to pyocyanin in an apparent two-step reaction catalyzed by the adenosylmethionine dependent methyltransferase PhzM and the flavin dependent hydroxylase, PhzS (*11, 14*). The *phzM* and *phzS* genes flank the core phenazine operon on the *P. aeruginosa* genome. We recently reported the crystal structure of PhzM and showed that PhzM is active only in the presence of PhzS, suggesting that an, at least transient, interaction between the two enzymes is required for pyocyanin production (*11*). Evidence also suggests that the putative intermediate, 5-methyl-PCA, is unstable and that a mechanism has evolved to ensure efficient conversion of PCA to pyocyanin. Furthermore, 5-methyl-PCA is an intermediate in the biosynthesis of another phenazine, aeruginosin A (*15*). Sequestration therefore may be part of a mechanism that partitions the intermediate in order to control the relative amounts of downstream products.

In this article, we report the crystal structure of PhzS, a flavin dependent hydroxylase that catalyzes the final step in pyocyanin biosynthesis, the oxidative decarboxylation of 5-methyl-PCA. Analysis of the structure reveals that PhzS is structurally similar to the family of flavin dependent hydroxylases that includes *p*-hydroxybenzoate hydroxylase (PHBH (*16*)), 3-hydroxybenzoate hydroxylase (3HBH; (*17*)), phenol hydroxylase (*18*), and the rebaccamycin biosynthetic enzyme, RebC (*19*). Biochemical analysis confirms that PCA is readily converted to pyocyanin by the combined action of PhzM and PhzS, although we have been unable to isolate a stable PhzM-PhzS complex. Kinetic data shows, however, that the rate of pyocyanin production is maximized when equimolar amounts of PhzS and PhzM are present.

PhzS may share more than a common fold with 3HBH and especially, RebC. The substrate binding site of PhzS appears to be accessible via a tunnel on the opposite side of PhzS from where NADH interacts with the flavin cofactor. A similar substrate binding scenario has been proposed for 3HBH and RebC. The mechanism of association and catalysis by a PhzM-PhzS complex, where a reactive intermediate is passed from the PhzM active site to the PhzS active site, would be simplified if NADH did not have to access a buried interface in order to reduce the flavin cofactor after substrate binding. Evidence further suggests that RebC, like PhzM, acts on an unstable intermediate produced, in that pathway, by RebP. A unique model of substrate binding has been postulated for RebC that could be shared by PhzS and that could accommodate a PhzM-PhzS complex in the conversion of PCA to pyocyanin. Mechanistically, PhzS may be unique among aromatic hydroxylases. An electron-poor substrate such as 5-methyl PCA is unlikely to participate in an electrophilic substitution reaction. Thus, PhzS either employs a novel means of substrate activation or it uses an entirely different mechanism to generate pyocyanin.

Table 1: Data Collection Statistics

| | |
|---|---|
| space group | *I*222 |
| cell parameters (*a*, *b*, *c*) (Å) | 63.5, 64.9, 182.0 |
| wavelength of data collection (Å) | 0.9792 |
| no. of measured intensities | 188721 |
| no. of unique reflections | 14742 |
| resolution of data (Å) | 30−2.4 |
| highest resolution shell (Å) | 2.49−2.40 |
| $R_{sym}$ (overall/high resolution shell) | 0.088/0.272 |
| completeness (%) (overall/high resolution shell) | 96.7/80.3 |
| redundancy (overall/high resolution shell) | 12.8/8.4 |
| mean $I/\sigma$ (overall/high resolution shell) | 23.2/5.2 |

## MATERIALS AND METHODS[2]

*Protein Expression and Purification.* The cloning, expression, and purification of PhzS have been previously reported (*11*). Selenomethionine (SeMet) substituted PhzS was expressed in *E. coli* strain B834(DE3), a methionine auxotroph, by growing the bacteria in M9 minimal media supplemented with selenomethionine. Purification procedures were unchanged except that 10 mM $\beta$-mercaptoethanol was added to the lysis buffer and to subsequent steps. For storage, SeMet-PhzS was dialyzed against 50 mM Bis-Tris, 1 mM DTT (pH 6.5), concentrated to ~15 mg/mL, and stored at −80 °C.

*Crystallization.* Crystals of SeMet-PhzS were grown at room temperature by the microbatch method under oil. Initial conditions were identified by high-throughput robotic screening (*20*). Crystals large enough for data collection were grown by mixing equal volumes of SeMet-PhzS, in storage buffer, and a solution containing 19% (w/v) polyethylene glycol 400, 0.10 M ammonium nitrate, and 0.10 M sodium acetate in the center well of a Chryschem (Hampton) 24-well sitting drop crystallization tray. Total drop volume was 6 $\mu$L. The drop was covered with paraffin oil immediately after mixing. Crystals formed in 2−4 days and grew as irregular yellow plates. Quality crystals of both native and SeMet-PhzS were very difficult to obtain. The data from the SeMet crystal used at the synchrotron was substantially better than any other PhzS data set collected to date; therefore, the structure reported here is of SeMet substituted PhzS.

*Data Collection.* Single-wavelength anomalous diffraction (SAD) data for the selenomethionine protein were collected at Brookhaven National Laboratory on beamline X29 using a wavelength of 0.9792 Å. Statistics are shown in Table 1. Crystals were frozen prior to data collection and stored in liquid nitrogen. No additional cryoprotectant was used. Diffraction data were processed with HKL2000 (*21*).

*Structure Determination and Refinement.* After data processing, the Matthews coefficient (2.35) indicated that there was one molecule of PhzS in the asymmetric unit cell. Using the SAD data for the SeMet labeled protein, six selenium sites were found by SHELXD (*22*). The sites were then used in SOLVE/RESOLVE to produce an initial electron density map (*23*). This map was examined using the graphics program COOT and judged to be of good quality (*24*). Using

[2] Certain commercial materials, instruments, and equipment are identified in this article in order to specify the experimental procedure as completely as possible. In no case does such identification imply a recommendation or endorsement by the National Institute of Standards and Technology nor does it imply that the materials, instruments, or equipment identified are necessarily the best available for the purpose.

Table 2: Refinement Statistics

| | |
|---|---|
| resolution limits (Å) | 20.0−2.40 |
| number of reflections used | 13593 |
| *R*-factor (overall/high resolution shell) | 0.194/0.232 |
| $R_{free}$ (overall/high resolution shell) | 0.262/0.347 |
| number of water molecules | 54 |
| rms deviation bond length (Å) | 0.015 |
| rms deviation angle (°) | 1.70 |
| average B main chain/side chain/water (Å$^2$) | 32.8/34.3/29.4 |

the anomalous data to 2.9Å with the iterative building script (www.solve.lanl.gov), which includes cycles of density modification and automated model building by RESOLVE and molecular refinement by REFMAC5 (*25*), 273 of the 402 residues were built, and 89 side chains were placed. COOT was used to visually examine, adjust, and expand the model, and REFMAC5 was used to refine the model between building sessions. At an intermediate stage, a second round of automated model building with the SAD phases and the current model, was used to confirm and extend the model. The final statistics are shown in Table 2. The final model includes residues 4−379. COOT was used to validate the final model. In a Ramachandran plot, 94.1% of the residues are in the preferred regions, and 5.9% are in the allowed regions.

*Modeling.* Comparative modeling methods using chemical intuition and a viable interaction strategy have been applied to build a model that simulates the structure of PhzS in complex with 5-methyl-PCA. The positions and orientations of FAD and 5-methyl-PCA in the active site were primarily based on the X-ray structure of the previously reported structure of chromopyrrolic acid-soaked RebC with bound 7-carboxy-K252c ((*19*); PDB code 2R0G). 2R0G was first superimposed on our presently reported PhzS structure. 5-methyl-PCA was then added to the PhzS structure using the program COOT (*24*). The initial orientations of FAD and 5-methyl-PCA in the model of PhzS were also established manually using COOT. The model of 5-methyl-PCA in the active site of PhzS was initially subjected to rigid body minimization with no experimental X-ray term. Residual strain in the model of the substrate plus the enzyme was relieved by conjugate gradient minimization, with no experimental X-ray term, and with the inclusion of all water molecules, using CNS 1.1 (*26*). Minimizations were carried out with a dielectric constant of 1.0. The optimized structure was analyzed with COOT (and statistical tools therein (*24*)) and PROCHECK (*27*). The rmsd for all Cα atoms of the minimized PhzS model with respect to the experimental model was 0.5 Å.

*Analysis of Enzymatic Activities.* PCA was purified from cultures of *P. fluorescens* according to the method of Gurusiddaiah et al. (*28*). Authentic pyocyanin was produced by photo-oxidative hydroxylation of phenazine methosulfate (Sigma (*29*)). 9-chloro-PCA was synthesized as previously described (*30*). Conversion of PCA to pyocyanin by PhzM and PhzS was monitored continuously, at 690 nm, or discontinuously by HPLC analysis of chloroform extracted reaction products. A standard continuous assay was defined in order to provide a benchmark against which other results can be compared. The standard assay contained 50 mM Tris (pH 7.8), 0.5 mM NADH, 0.30 mM PCA, 0.50 mM SAM, 250 nM PhzM, and 250 nM PhzS. Kinetic analyses were conducted at 25 °C.

The stoichiometry and strength of the putative PhzM-PhzS complex was evaluated by examining the rate of pyocyanin formation while varying the concentration of one enzyme (PhzM) and keeping the concentration of the other (PhzS) fixed. Data were fit to a quadratic function (eq 1) where *A* is the titration amplitude, and [*S*] and [*M*] are the concentrations of PhzS and PhzM.

$$y = \frac{A * ((K_d + [S] + [M]) - \left(\sqrt{(K_d + [S] + [M])^2 - 4[S][M]}\right))}{2[S]} \quad (1)$$

*Regiochemistry of Hydroxylation and Analysis of Products from Reactions in $D_2O$.* The PCA analogue 9-chloro-PCA (*30*) was used to assess the regiochemical specificity of PhzS. A 2 mL reaction containing 1 mM 9-chloro-PCA, 2 μM PhzM, 2 μM PhzS, 250 μM NADH, and 2 mM SAM was aerated by gentle shaking at room temperature for 1 h. The pH of the reaction was then adjusted to ∼12 with NaOH, and the reaction was extracted with two 4 mL volumes of chloroform. The combined chloroform extracts were evaporated to dryness under a stream of nitrogen gas, and the residue was resuspended in 0.5 mL of a 60:40 mixture of acetonitrile and 0.1% TFA in water and analyzed using a Mariner electrospray ionization mass spectrometer (Applied Biosystems). A control reaction containing PCA was performed simultaneously to verify that it could be converted to pyocyanin in these assays. A similar scheme was used to evaluate whether deuterium could be incorporated into nonexchangeable positions on pyocyanin. In these cases, reactions were run in deuterated buffer made by dissolving *d11*-Tris in 99.9% $D_2O$ and adjusting the pH with *d4*-acteic acid. All reaction components were dissolved in this buffer prior to assembling the 2 mL reaction as described above.

*Instrumental Methods.* UV/visible spectra were acquired at 25 °C using a Cary 4 double beam spectrophotometer. HPLC was used to separate and identify reactions products on the basis of retention time. A 4.6 × 100 mm XTerra MS C18 reversed phase column (Waters) was used in conjunction with a Gilson binary gradient HPLC system to analyze products. Pyocyanin and 9-chloro-pyocyanin were detected at 280 nm using a mobile phase consisting of 0.01% TFA (Solvent A) and 0.01% TFA in acetonitrile (Solvent B). The following method was used: 0−5 min, 5% solvent B; 5−13 min, a linear gradient from 5% solvent B to 100% solvent B. Pyocyanin eluted at 5.73 min, and 9-cholor-pyocyanin eluted at 7.36 min. The flow rate used was 1 mL/minute, and analytical injections were 20 μL or less.

## RESULTS AND DISCUSSION

*Overall Structure.* The PhzS polypeptide has 402 amino acids, and the enzyme exists as a monomer in solution (*11*). The final model of SeMet-PhzS contains residues 4−379, one FAD molecule, and 54 water molecules. No electron density is present for the C-terminal 23 residues, suggesting that they are disordered. PhzS folds into a complex, two domain structure. The domains are not formed from contiguous portions of the primary structure, rather, the polypeptide meanders between domains. Domain 1 consists of residues 3−72, 99−177, and 297−379, while domain 2 consists of residues 73−98 and 178−296. A similar pattern is seen in

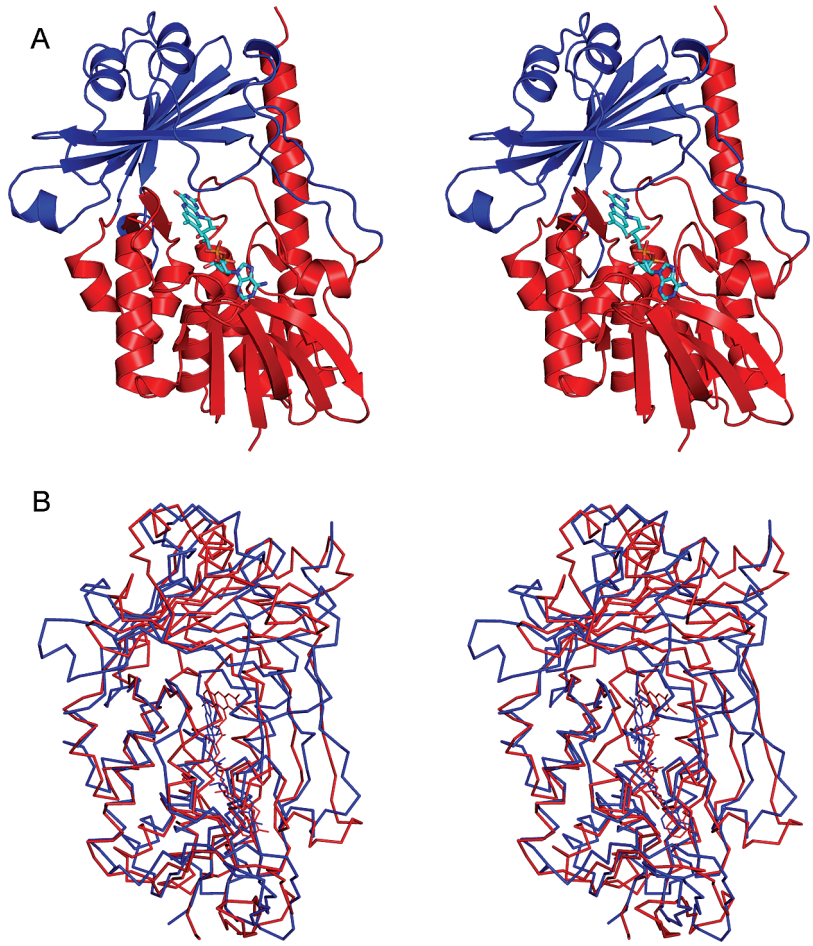


FIGURE 2: PhzS is a flavin dependent monooxygenase structurally related to *p*-hydroxybenzoate hydroxylase. (A) Stereo ribbon diagram of PhzS illustrating the overall fold of the protein. Domains 1 and 2 are colored red and blue respectively. (B) Superposition of the Cα atoms of PhzS (blue) and PHBH (red; 1K0I), shown in stereo view.

other flavin dependent hydroxylases as well. Domain 1, the larger of the two domains, is built around a five stranded parallel $\beta$-sheet, which is sandwiched between a three stranded antiparallel $\beta$-sheet and four α-helices (Figure 2). Nearly all contacts with the FAD cofactor are contributed by domain 1 of PhzS, and the ADP portion of the cofactor interacts exclusively with domain 1. Domain 2 of PhzS features a large seven stranded mostly antiparallel $\beta$-sheet that defines a significant portion of the substrate binding cavity. Three small α-helices pack against the outside of this $\beta$-sheet. A long loop region (residues 245−258) between two of these helices folds over the edge of the $\beta$-sheet and forms a lid over the riboflavin portion of the FAD cofactor (Figures 2A, 4A). Trp253 anchors the loop in place by forming a stacking interaction with the isoalloxazine ring of FAD (Figure 3A).

*Structure Relatives.* Table 3 summarizes the similarities between PhzS and selected structural homologues. The core of the hydroxylase fold, consisting of domains 1 and 2, encompasses ~325 residues. Many flavin dependent hydroxylases have an additional domain that typically corresponds to the C-terminal portion of the amino acid sequence, often some 200 plus residues. In some cases, the domain is involved in oligomerization, and in other cases, its function is unclear. In PHBH, the domain is a small α-helical region that corresponds to the dimer interface. The disordered C-terminus of PhzS makes it difficult to judge whether the region could be characterized as a separate domain or what its role is given that PhzS is a monomer. Nonetheless, PhzS most closely resembles PHBH in terms of chain length, although this may be of little consequence in terms of the evolutionary path each has taken to optimize catalysis.

*Active Site.* FAD is bound in a cleft comprising residues from both domains of the enzyme (Figures 2A and 4A). The ADP portion of the cofactor adapts a conformation that closely mirrors what is seen in other similar proteins. The adenosine ring is situated near the end of $\beta$1, the central strand of the first $\beta$-sheet. This is a typical ligand binding site in α/$\beta$ hydrolase domains, which are characterized by a $\beta$-sheet structure similar to the one seen in PhzS. A conserved acidic residue, Glu35, forms a strong hydrogen-bonding interaction with the 2′ and 3′ hydroxyl groups of the ribose ring. Asp 310 interacts with the ribityl O2 hydroxyl and a $\beta$-phosphoryl oxygen, the latter via its amide nitrogen. Arg106 has multiple interactions with the cofactor and may play a large role in orienting the flavin (Figure 3A). The guanidino group of Arg106 is stacked against the *si* face of the flavin, and hydrogen bonds are observed between NE of Arg106 and the O3 hydroxyl of the ribityl chain, and between NH2 of Arg106 and O5, an α-phosphoryl oxygen atom. These three interactions appear to be major determinants of the observed flavin conformation. Trp253 stacks against the *re* side of the flavin, creating essentially a sandwich arrangement in which the flavin is held in place by the indole

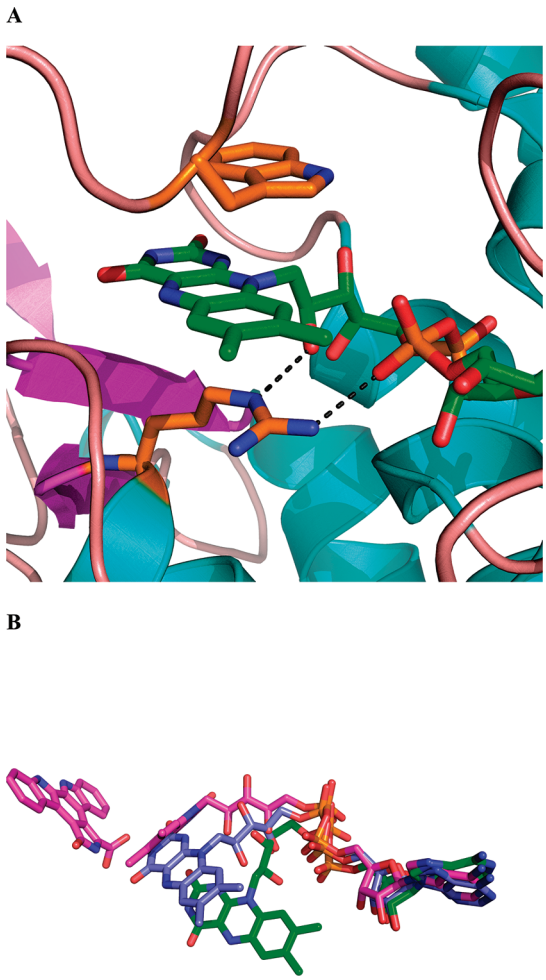


FIGURE 3: Factors affecting the flavin orientation and conformation in PhzS and comparison with the flavin conformations observed in the structural homologue RebC. (A) Close up view of the flavin binding site of PhzS illustrating factors that contribute to the observed flavin position. Trp253 and Arg106 sandwich the isoalloxazine ring of the flavin. Hydrogen bonds between NE of Arg106 and O3 of the ribityl chain (2.66 Å) and between NH2 of Arg106 and a phosphoryl oxygen (2.97 Å) are shown as dashed lines. (B) Flavin conformations observed in PhzS (green), apo RebC (blue; 2R0C), and liganded RebC (pink; 2R0G). The flavin bound to PhzS adopts a highly contorted out conformation, relative to similar enzymes, due to the interactions of the flavin with Arg106 and Trp253. Binding of the RebC substrate triggers a movement of the flavin to the in position.

ring of the tryptophan and the guanidino group of the arginine. A very similar arrangement is seen in RebC where the isoalloxazine ring is sandwiched between Arg46 and Trp276. Motion of the isoalloxazine ring of FAD, in flavin dependent hydroxylases, is an established element of catalysis (*16*). Substrate binding triggers a rotation of the flavin around its ribityl chain that moves the isoalloxazine ring from an out position to an in position that is closer to the substrate binding site and that is shielded from solvent. In unliganded PhzS, the flavin is in the out position, as expected. Indeed, the PhzS flavin is significantly more bent, in its out position, than are flavins from related structures (Figure 3B).

*Modeling of the Enzyme−Substrate Complex.* Thus far we have been unable to crystallize PhzS with a bound ligand. However, the location of the substrate binding site of PhzS can be inferred from an examination of structurally homologous proteins. Superimposing the structure of PhzS with the liganded structures of PHBH (1K0I), RebC (2R0G), and

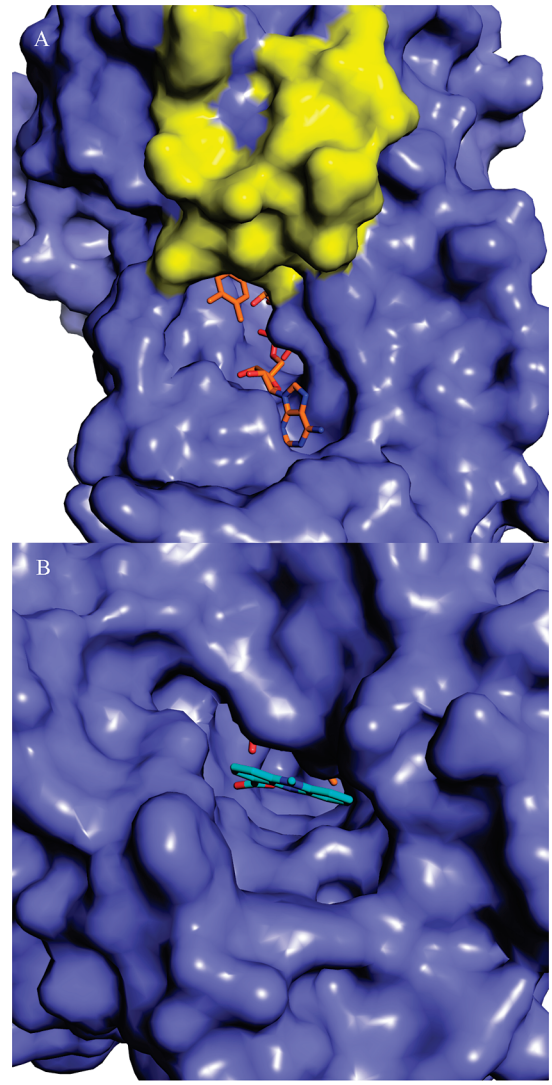


FIGURE 4: Location, accessibility, and relative size of the PhzS active site. (A) Surface representation of PhzS with the FAD cofactor shown as a stick model. The loop (residues 245−258) that includes Trp253 and that forms a partial lid over the isoalloxazine ring of FAD is shown as a yellow surface. (B) Surface representation of PhzS rotated approximately 180° from the view shown in A and showing the substrate binding cavity, which is occupied by a stick model of 5-methyl-PCA.

Table 3: PhzS Structural Homologues

| PDB entry | protein | Z score[a] | rmsd (Å) for aligned Cα | no. of aligned residues | % sequence identity |
|---|---|---|---|---|---|
| 1K0I | PHBH | 30.9 | 3.3 | 340 | 17 |
| 1PN0 | phenol hydroxylase | 33.2 | 2.8 | 337 | 20 |
| 2R0C | RebC | 24.6 | 2.9 | 306 | 22 |
| 2DKH | 3-hydroxybenzoate hydroxylase | 23.1 | 2.7 | 330 | 18 |
| 2QA1 | polyketide oxygenase, PgaE | 25.6 | 3.2 | 321 | 18 |
| 2OAL | tryptophan halogenase | 26.6 | 3.2 | 321 | 13 |

[a] All calculations made using DaliLite (*37*).

3HBH (2DKH) identified the likely site of 5-methyl PCA binding. Manual docking of a model of the substrate followed by energy minimization yielded a reasonable model of how 5-methyl PCA may bind to PhzS. Figures 4B and 5 illustrate

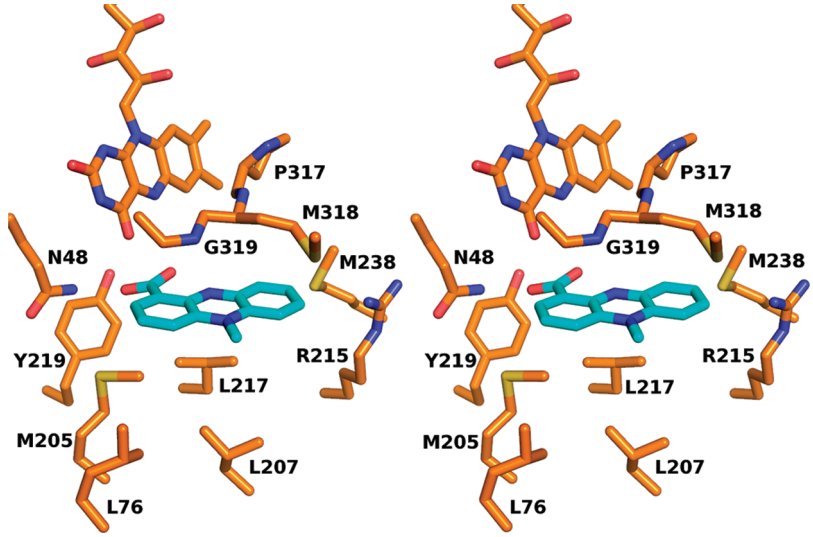


FIGURE 5: Stereo representation depicting a model of 5-methyl-PCA bound to the PhzS active site. The carboxyl group of PCA is predicted to be within hydrogen-bonding distance of the side chains of Asn48 and Tyr219. The predicted binding site is otherwise dominated by hydrophobic side chains. The model was generated as described in the text.

the predicted substrate binding site of PhzS and suggest which residues are candidates for interaction with the substrate. As expected, the binding site is dominated by hydrophobic residues (Figure 5). The side chain amide of Asn48 and the phenolic oxygen of Tyr219, however, are predicted to be within hydrogen-bonding distance of the C1 carboxylate of 5-methyl PCA and may play a role in catalysis. In the current model, no interaction is seen between the protein and the quaternary amine of 5-methyl PCA. It is likely, however, that one or more residues, either from the disordered C-terminus or from PhzM, will interact with the quaternary methyl group of the substrate. The distance between C4a of the flavin and C1 of the model of 5-methyl PCA is 5.4 Å. This distance is similar to what is seen between analogous atoms in other aromatic hydroxylases (*19*).

*Catalytic Activity of PhzS.* We previously reported that PCA can only be converted to pyocyanin when both PhzM and PhzS are present and that PhzM is inactive alone. Additionally, we reported that PhzS, like many flavin dependent hydroxylases, will act on other substrates but with poor efficiency (*11*). This inefficiency is characterized by excess NADH consumption and subsequent hydrogen peroxide formation during futile catalytic cycles. Available evidence suggests PhzM and PhzS form a transient complex that activates PhzM and ensures pyocyanin formation by preventing the release of the apparently unstable 5-methyl-PCA intermediate.

*Regiochemistry of Hydroxylation.* Formation of pyocyanin involves both a decarboxylation and a hydroxylation. Most characterized PhzS homologues, such as PHBH, catalyze hydroxylation at unsubstituted carbon atoms; however, a few examples are known that involve simultaneous decarboxylation. Examples include salicylate hydroxylase and 6-hydroxynicotinate hydroxylase (*31, 32*). In both cases, the substrates are single ring structures, and chemistry occurs at a single carbon. The RebC catalyzed reaction appears to involve a decarboxylation as well; however, that substrate is more complex than the PhzS substrate, and as with PhzS, many of the details are unclear including the specific identity of the substrate. In the case of PhzS, the tricyclic structure of the substrate raises some questions. While the carboxyl group obviously departs from C1, the hydroxylation could, in principle, occur at either C1 or C9, in either case yielding pyocyanin. In order to assess whether a single reaction center was involved in the hydroxylation and decarboxylation reactions, the products of a reaction initially containing the alternative substrate 9-chloro-PCA were analyzed. The color of the reaction solutions changed quickly from yellow to greenish blue, suggesting that the compound was in fact a substrate. Mass spectrometry revealed that a compound consistent with 9-chloropyocyanin (Figure 6A; $m/z_{calcd}$ = 245.05; $m/z_{obs}$ = 244.96) or a structural isomer was formed in these reactions and confirmed that chemistry does not occur at C9, and strongly suggested that all chemistry occurs at C1, as anticipated. Control reactions, initially containing PCA, produced pyocyanin as expected (Figure 6B; $m/z_{calcd}$ = 211.09; $m/z_{obs}$ = 210.99).

*Catalytic Mechanism.* Given the structural similarities between PhzS and the PHBH family of aromatic hydroxylases (Table 3) and the wealth of mechanistic data available on these enzymes, they represent a reasonable starting point for an examination of the mechanism of catalysis by PhzS. The early steps in catalysis, reduction of the flavin cofactor by NADH and the reaction of the reduced flavin with molecular oxygen, which generates the C4a-flavin hydroperoxide, are likely quite similar. However, after the formation of the activated oxygen species, the details of the PhzS catalyzed reaction become less obvious.

PHBH, the prototypical aromatic hydroxylase, uses an electrophilic substitution mechanism in which the substrate, *p*-hydroxybenzoate, is activated for nucleophilic attack on a C4a-flavin hydroperoxide. The nucleophilicity of the substrate is enhanced by deprotonation of the substrate hydroxyl group by an active site hydrogen bonding network (*33*). In the case of PhzS, the electron deficient substrate, 5-methyl PCA, is expected to be a very poor nucleophile and thus unlikely to react via an electrophilic substitution mechanism (Figure 8, path A) without some assistance analogous to the PHBH hydrogen bond network. 5-methyl PCA lacks a readily ionizable functional group; however, proton abstraction from the quaternary methyl group of the substrate by a basic active site residue could generate a species with

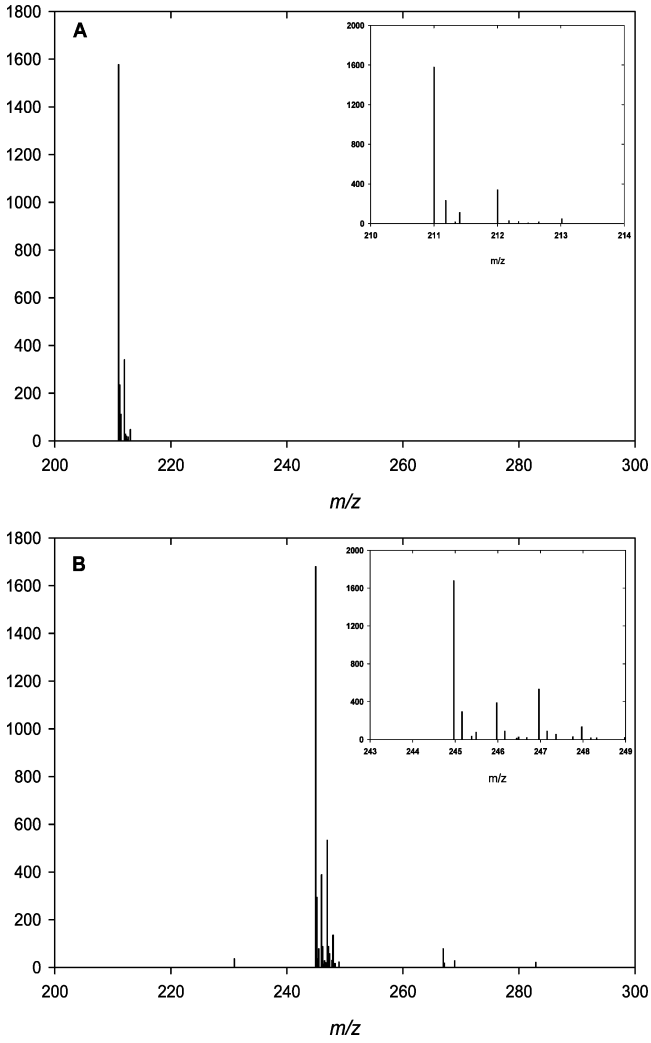


FIGURE 6: Mass spectral analysis of products extracted from PhzM-PhzS catalyzed reactions initially containing either PCA or 9-chloro-PCA suggests that a single carbon is involved in the decarboxylation/hydroxylation catalyzed by PhzS. (A) Pyocyanin is the only chloroform soluble product found in control reactions with PCA. (B) A compound consistent with the mass and isotopic distribution of 9-chloropyocyanin is found in reactions containing 9-chloro-PCA.

increased electron density at C1. The possibility that PhzS uses such a mechanism was tested by converting PCA to pyocyanin in $D_2O$ and, using mass spectrometry, looking for a product containing deuterium, which would have been incorporated upon reprotonation of the methyl group. No deuterium incorporation was evident. Pyocyanin produced in deuterated solvent had the same mass ($m/z_{calcd} = 211.09$; $m/z_{obs} = 210.91$) as that of pyocyanin produced in simultaneously run control reactions in $H_2O$ ($m/z_{calcd} = 211.09$; $m/z_{obs} = 210.92$), suggesting that the enzyme does not use a mechanism that involves proton abstraction from the quaternary methyl group to increase electron density at C1. These findings are consistent with the structure of PhzS presented here. Figures 4 and 5 show that no residues appear to be positioned to act as a general base in a proton abstraction step. It remains possible that elements of PhzM, in a PhzM-PhzS complex, or the disordered tail of PhzS could interact with the substrate. However, the observation that deuterium is not incorporated suggests general base catalysis is not part of the mechanism.

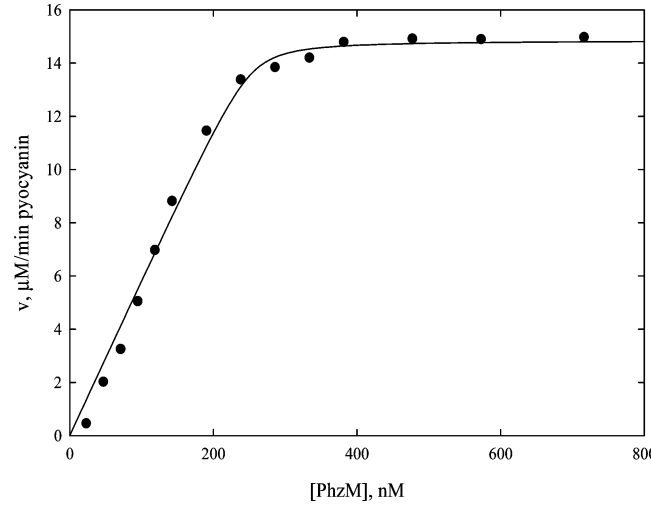


FIGURE 7: Analysis of the rate of pyocyanin formation from a PhzM-PhzS mixture as a function of PhzM concentration. The rate increases linearly until a one-to-one ratio of PhzM to PhzS is reached and then plateaus to a constant rate. This observation suggests that pyocyanin formation involves a high affinity, 1:1 PhzM-PhzS complex. Pyocyanin formation was monitored at 690 nm in assays containing 240 nM PhzS, 560 $\mu$M NADH, 300 $\mu$M SAM, 325 $\mu$M PCA, and various amounts of PhzM. The data were fit to eq 1 and illustrate that the maximum initial rate of pyocyanin formation in these assays is achieved at a 1:1 ratio of PhzM:PhzS. The analysis implies that if the change in rate is attributable to a complex then a dissociation constant of approximately 2 nM describes the interaction of PhzM and PhzS. The concentration of PhzS in the reaction determined from the fit is 253 $\pm$ 10 nM.

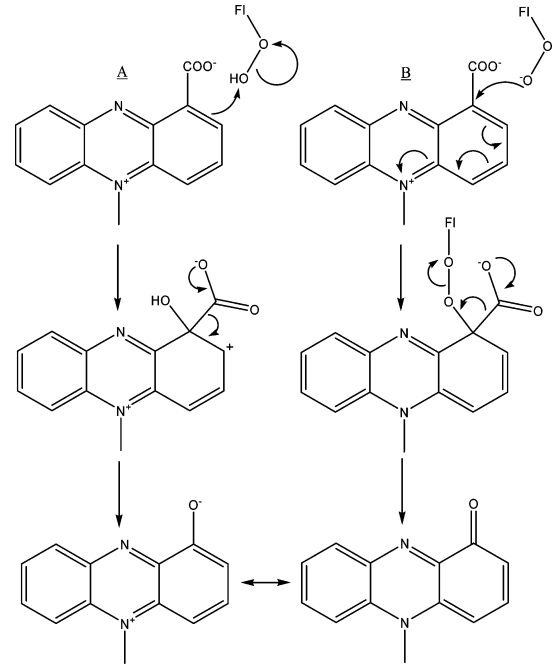


FIGURE 8: Two possible mechanisms for the PhzS catalyzed formation of pyocyanin. Path A depicts an electrophilic substitution mechanism that PHBH and other structural homologues of PhzS have been shown to use. Path B depicts an alternate mechanism involving nucleophilic attack by the C4a-flavin peroxide on the relatively electrophilic 5-methyl-PCA substrate. The products shown are interconvertible resonance forms of pyocyanin (*1*).

A second possibility is that PhzS is structurally similar to PHBH but mechanistically dissimilar. Flavin monooxygenases such as cyclohexanone mono-oxygenase and bacterial luciferase, for example, catalyze reactions in which a C4a-

flavin peroxide is the nucleophile rather than the eletrophile as discussed above (*34, 35*). Indeed, if not for the observed structural similarity between PHBH and PhzS, perhaps a more plausible scenario would be that PhzS catalyzes the nucleophilic attack of the C4a-flavin peroxide on a relatively electrophilic substrate, 5-methyl PCA (Figure 8, path B). While the lack of deuterium incorporation in pyocyanin does not favor the electrophilic mechanism discussed above, additional experimentation is required before either mechanism can be discounted.

*Stoichiometry of the PhzM-PhzS Complex.* Analysis of initial reaction velocities shows that the maximum rate of pyocyanin formation is achieved when equal molar amounts of PhzM and PhzS are present (Figure 7). An excess of either enzyme does not enhance the rate of pyocyanin formation, and no lag was observed in the assays at any enzyme concentration. Together, these observations corroborate the notion that a physical interaction between PhzM and PhzS is required and that no 5-methyl-PCA is released into solution. The data in Figure 7 also predicts that, if in fact activity is stimulated by complex formation, that PhzM and PhzS are tightly associated. However, the factor or event that triggers association is unclear.

While no structure is yet available for a PhzM-PhzS complex, the individual structures of these enzymes contain sufficient information to develop a reasonable hypothesis about how they interact and how efficient pyocyanin biosynthesis might be maintained. The structure of PhzS suggests that the substrate, 5-methyl-PCA, gains access to the active site through a back door rather than negotiating past the flavin as *p*-hydroxybenzoate does in PHBH (*36*). 3HBH and RebC are also thought to have separate entrances for their substrates. Interestingly, in RebC, like in PhzS, portions of the structure close to the substrate binding site are disordered in the absence of substrate. Upon binding substrate via this back door, residues 354−363 of RebC form an ordered helix that appears to lock the substrate into the active site (*19*). Like RebC, unliganded PhzS also has a disordered region (residues 380−402) near the substrate binding site, which might become ordered upon substrate binding. However, it is also possible that this disordered region interacts with PhzM since it is close to the entrance to the PhzS active site, or it may be involved in both processes. A reasonable scenario consistent with available data would involve the juxtaposition of PhzM and PhzS active sites such that the intermediate is not released into solution but transferred directly between active sites. This model of substrate binding makes a PhzM-PhzS complex more plausible because the NADH binding site of PhzS will not likely be buried as it would be if PhzS bound substrates in the same way that PHBH does. The disordered C-terminus of PhzS could be involved in the recognition of PhzM by becoming ordered upon interaction with PhzM, or it may be involved in the dissociation of the transient complex after the intermediate is passed between active sites if a conformational change in PhzS occurs.

## CONCLUSIONS

The structure of PhzS reveals that it is a flavin dependent aromatic hydroxylase that is structurally similar to PHBH, the archetypal flavin dependent aromatic hydroxylase. The structure of PhzS suggests that it binds substrate via a tunnel on the protein surface that is distant from the cavity where FAD is located. The RebC hydroxylase, which functions in rebeccamycin biosynthesis, has been shown to bind its substrate in this fashion. Both PhzS and RebC exhibit disorder in the vicinity of the substrate binding site in the unliganded state. The disordered region in RebC becomes ordered upon ligand binding, and this has been proposed to be an integral part of the substrate recognition process. We propose that in PhzS, the disordered region could perform the same function, recognizing substrate, or a similar function, recognizing PhzM in order to form a transient PhzM-PhzS complex. Biochemical evidence suggests that the PhzM-PhzS complex contains equal molar amounts of each protein. Since PhzM is a dimer, a $PhzM_2$-$S_2$ complex is likely to be the active species.

## REFERENCES


1. Swan, G. A., and Felton, D. G. I. (1957) Phenazines, in *The Chemistry of Heterocyclic Compounds* (Weissberger, A., Ed.), Interscience Publishers, New York.
2. Laursen, J. B., and Nielsen, J. (2004) Phenazine natural products: biosynthesis, synthetic analogues, and biological activity. *Chem. Rev. 104*, 1663–1686.
3. Mavrodi, D. V., Blankenfeldt, W., and Thomashow, L. S. (2006) Phenazine compounds in fluorescent *Pseudomonas* spp. biosynthesis and regulation. *Annu Rev Phytopathol. 44*, 417–445.
4. Mavrodi, D. V., Ksenzenko, V. N., Bonsall, R. F., Cook, R. J., Boronin, A. M., and Thomashow, L. S. (1998) A seven-gene locus for synthesis of phenazine-1-carboxylic acid by *Pseudomonas fluorescens* 2−79. *J. Bacteriol. 180*, 2541–2548.
5. Lau, G. W., Hassett, D. J., Ran, H., and Kong, F. (2004) The role of pyocyanin in *Pseudomonas aeruginosa* infection. *Trends Mol. Med. 10*, 599–606.
6. Lau, G. W., Ran, H., Kong, F., Hassett, D. J., and Mavrodi, D. (2004) *Pseudomonas aeruginosa* pyocyanin is critical for lung infection in mice. *Infect. Immun. 72*, 4275–4278.
7. Look, D. C., Stoll, L. L., Romig, S. A., Humlicek, A., Britigan, B. E., and Denning, G. M. (2005) Pyocyanin and its precursor phenazine-1-carboxylic acid increase IL-8 and intercellular adhesion molecule-1 expression in human airway epithelial cells by oxidant-dependent mechanisms. *J. Immunol. 175*, 4017–4023.
8. Lyczak, J. B., Cannon, C. L., and Pier, G. B. (2000) Establishment of *Pseudomonas aeruginosa* infection: lessons from a versatile opportunist. *Microbes Infect. 2*, 1051–1060.
9. O'Malley, Y. Q., Reszka, K. J., Spitz, D. R., Denning, G. M., and Britigan, B. E. (2004) *Pseudomonas aeruginosa* pyocyanin directly oxidizes glutathione and decreases its levels in airway epithelial cells. *Am. J. Physiol. Lung Cell Mol. Physiol. 287*, L94–103.
10. Parsons, J. F., Song, F., Parsons, L., Calabrese, K., Eisenstein, E., and Ladner, J. E. (2004) Structure and function of the phenazine biosynthesis protein PhzF from *Pseudomonas fluorescens* 2−79. *Biochemistry 43*, 12427–12435.
11. Parsons, J. F., Greenhagen, B. T., Shi, K., Calabrese, K., Robinson, H., and Ladner, J. E. (2007) Structural and functional analysis of the pyocyanin biosynthetic protein PhzM from *Pseudomonas aeruginosa*. *Biochemistry 46*, 1821–1828.
12. Parsons, J. F., Calabrese, K., Eisenstein, E., and Ladner, J. E. (2004) Structure of the phenazine biosynthesis enzyme PhzG. *Acta Crystallogr., Sect. D 60*, 2110–2113.
13. Parsons, J. F., Calabrese, K., Eisenstein, E., and Ladner, J. E. (2003) Structure and mechanism of *Pseudomonas aeruginosa* PhzD, an isochorismatase from the phenazine biosynthetic pathway. *Biochemistry 42*, 5684–5693.
14. Mavrodi, D. V., Bonsall, R. F., Delaney, S. M., Soule, M. J., Phillips, G., and Thomashow, L. S. (2001) Functional analysis of genes for biosynthesis of pyocyanin and phenazine-1-carboxamide from *Pseudomonas aeruginosa* PAO1. *J. Bacteriol. 183*, 6454–6465.
15. Hansford, G. S., Holliman, F. G., and Herbert, R. B. (1972) Pigments of *Pseudomonas* species. Part IV. In vitro and in vivo conversion of 5-methylphenazinium-1-carboxylate into aeruginosin A. *J. Chem. Soc., Perkin Trans. 1*, 103–105.

16. Gatti, D. L., Palfey, B. A., Lah, M. S., Entsch, B., Massey, V., Ballou, D. P., and Ludwig, M. L. (1994) The mobile flavin of 4-OH benzoate hydroxylase. *Science 266*, 110–114.
17. Hiromoto, T., Fujiwara, S., Hosokawa, K., and Yamaguchi, H. (2006) Crystal structure of 3-hydroxybenzoate hydroxylase from *Comamonas testosteroni* has a large tunnel for substrate and oxygen access to the active site. *J. Mol. Biol. 364*, 878–896.
18. Enroth, C., Neujahr, H., Schneider, G., and Lindqvist, Y. (1998) The crystal structure of phenol hydroxylase in complex with FAD and phenol provides evidence for a concerted conformational change in the enzyme and its cofactor during catalysis. *Structure 6*, 605–617.
19. Ryan, K. S., Howard-Jones, A. R., Hamill, M. J., Elliott, S. J., Walsh, C. T., and Drennan, C. L. (2007) Crystallographic trapping in the rebeccamycin biosynthetic enzyme RebC. *Proc. Natl. Acad. Sci. U.S.A. 104*, 15311–15316.
20. Luft, J. R., Collins, R. J., Fehrman, N. A., Lauricella, A. M., Veatch, C. K., and DeTitta, G. T. (2003) A deliberate approach to screening for initial crystallization conditions of biological macromolecules. *J. Struct. Biol. 142*, 170–179.
21. Minor, W., and Otwinowski, Z. (1997) In *Methods in Enzymology* (Carter, C. W., and Sweet, R. M., Eds.) pp307−326, Academic Press, New York.
22. Uson, I., and Sheldrick, G. M. (1999) Advances in direct methods for protein crystallography. *Curr. Opin. Struct. Biol. 9*, 643–648.
23. Terwilliger, T. C. (2003) Automated main-chain model building by template matching and iterative fragment extension. *Acta Crystallogr., Sect. D 59*, 38–44.
24. Emsley, P., and Cowtan, K. (2004) Coot: model-building tools for molecular graphics. *Acta Crystallogr., Sect. D 60*, 2126–2132.
25. Winn, M., Isupov, M., and Murshudov, G. N. (2001) Use of TLS parameters to model anisotropic displacements in macrololecular refinement. *Acta. Crystallogr., Sect. D 57*, 122–133.
26. Brunger, A. T., Adams, P. D., Clore, G. M., DeLano, W. L., Gros, P., Grosse-Kunstleve, R. W., Jiang, J. S., Kuszewski, J., Nilges, M., Pannu, N. S., Read, R. J., Rice, L. M., Simonson, T., and Warren, G. L. (1998) Crystallography & NMR system: A new software suite for macromolecular structure determination. *Acta Crystallogr., Sect. D 54*, 905–921.
27. Laskowski, R. A., and MacArthur, M. W. (1993) PROCHECK: a program to check the stereochemicalquality of protein structures. *J. Appl. Crystallogr. 26*, 283–291.
28. Gurusiddaiah, S., Weller, D. M., Sarkar, A., and Cook, R. J. (1986) Characterization of an antibiotic produced by a strain of *Pseudomonas fluorescens* Inhibitory to *Gaeumannomyces graminis* var *tritici* and *Pythium* spp. *Antimicrob. Agents Chemother. 29*, 488–495.
29. Halaka, F. G., Babcock, G. T., and Dye, J. L. (1982) Properties of 5-methylphenazinium methyl sulfate. *J. Biol. Chem. 257*, 1458–1461.
30. Rewcastle, G. W., and Denny, W. A. (1987) Unequivocal synthesis of phenazine-1-carboxylic acids: selective displacement of fluorine during alkaline borohydride reduction of N-(2-fluorophenyl)-3-nitroanthranilic acids. *Synth. Commun. 17*, 1171–1179.
31. Nakano, H., Wieser, M., Hurh, B., Kawai, T., Yoshida, T., Yamane, T., and Nagasawa, T. (1999) Purification, characterization and gene cloning of 6-hydroxynicotinate 3-monooxygenase from *Pseudomonas fluorescens* TN5. *Eur. J. Biochem. 260*, 120–126.
32. Wang, L. H., and Tu, S. C. (1984) The kinetic mechanism of salicylate hydroxylase as studied by initial rate measurement, rapid reaction kinetics, and isotope effects. *J. Biol. Chem. 259*, 10682–10688.
33. Entsch, B., Cole, L. J., and Ballou, D. P. (2005) Protein dynamics and electrostatics in the function of p-hydroxybenzoate hydroxylase. *Arch. Biochem. Biophys. 433*, 297–311.
34. Sheng, D., Ballou, D. P., and Massey, V. (2001) Mechanistic studies of cyclohexanone monooxygenase: chemical properties of intermediates involved in catalysis. *Biochemistry 40*, 11156–11167.
35. Fisher, A. J., Thompson, T. B., Thoden, J. B., Baldwin, T. O., and Rayment, I. (1996) The 1.5-A resolution crystal structure of bacterial luciferase in low salt conditions. *J. Biol. Chem. 271*, 21956–21968.
36. Wang, J., Ortiz-Maldonado, M., Entsch, B., Massey, V., Ballou, D., and Gatti, D. L. (2002) Protein and ligand dynamics in 4-hydroxybenzoate hydroxylase. *Proc. Natl. Acad. Sci. U.S.A. 99*, 608–613.
37. Holm, L., and Park, J. (2000) DaliLite workbench for protein structure comparison. *Bioinformatics 16*, 566–567.

BI702480T